RECONSTRUCTING HELENE'S SURFACE HISTORY – PLASTICS AND SNOW., O. M. Umurhan[1], A. D. Howard[2], J. M. Moore[1], P. Schenk[3] and O. L. White[1]. [1]NASA Ames Research Center, MS 245-3, Moffett Field, CA 94035-1000 (orkan.m.umurhan@nasa.gov), [2]University of Virginia, Department of Environmental Sciences, P.O. Box 400123, Charlottesville, VA 22904-4123, [3]Lunar and Planetary Institute, 3600 Bay Area Boulevard, Houston, TX 77058

Introduction: Helene poses many interpretive challenges. It is the co-orbiting (leading) Trojan moon of Dione with dimensions 43x36x28 km and an approximate location-varying surface gravity no more than 0.5 cm/s^2. The Dione system sits in the outer part of the E-ring which is composed of ionized ice grains emanating from Enceladus [1,2]. Helene's dimensions make it an interesting object to study in light of a *potential* post-Pluto encounter redirection of the New Horizons Mission *(pending funding)* to one of several recently identified candidate KBO's of similar size.

High resolution images of Helene taken by the Cassini spacecraft (42m/pix) shows indications of a surface undergoing geologic processes such as mass-wasting and erosion [1,3]. The landscape is characterized by broad 2-10 km scale depressions with large scale interior slopes no greater than 12^o. These basins appear to be the decayed remains of previous cratering events. Neighboring crater basins show narrowing of their shared septas and crater rims indicating slumping events. The surface materials (hereafter referred to as ``snow" or ``dust") are of relatively high reflectance suggesting material/grain sizes between 1 and 100 μm. Small craters appear mantled, suggesting recent accretional processes of some sort.

Most striking is the evidence for erosion and mass transport where thin elongated km-scale raised grooves (indicated by their relatively low albedo) border the aforementioned broad basins. Groove features appear to trace out downgradient paths suggesting mass flow patterning everywhere on the surface. Using digital elevation models we have developed, these grooves are found to display positive relief of 50-100m.

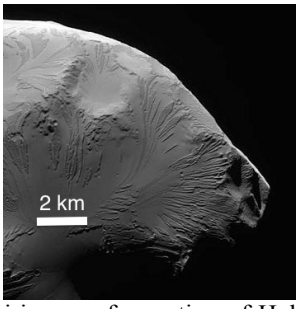

Fig. 1 Cassini image of a section of Helene's surface. The broad basins and grooved patterns clearly shown.

Hypothesis and Aims: Stress-strain laboratory testing of lunar regolith samples show that at low packing densities they behave like Non-Newtonian "Bingham" materials, i.e., having the plastic quality of candle-wax and glaciers [4]. This observation taken together with the above facts about Helene inspires us to *hypothesize that the mysterious smooth icy dust on Helene behaves as a non-Newtonian mass flow and is primarily responsible for the visible flow patterns seen on its low-gravity surface*.

Within this "plastic framework", our primary aim is to reconstruct Helene's surface dynamics by considering the outcome of differing historical scenarios including: (i) Steady "*weathering"* of the surface (perhaps due to micrometeorite impacts) where an ice "bedrock" is equivolumetrically converted into transportable snowy-dust, referred to also as "regolith". (ii) Steady "*accretion"* onto the surface of snow which subsequently transports, (iii) "*Catastrophic liberation"* meaning the transformation of a certain amount of bedrock into snowy transportable regolith as resulting from, for example, the impact of a relatively large meteor. The above scenarios are considered in tandem.

Model and Methods: We represent these processes through the following coupled nonlinear partial differential evolutionary model for the snowy dust regolith $h_r(x,y,t)$ and the underlying bedrock $h_b(x,y,t)$

$$\begin{aligned} \partial_t h_r &= \nabla\cdot\mathbf{q} + \dot{h}_a + \dot{h}_b, \\ \partial_t h_b &= -\dot{h}_b = -\dot{h}_w - \tau_0 \,|\mathbf{q}|, \end{aligned} \tag{1.1}$$

where the non-Newtonian mass flux vector is given by $\mathbf{q} \equiv \Delta\cdot\Xi(\Delta,h_r)\cdot\nabla h$, and the total elevation is defined by $h \equiv h_r + h_b$. The product quantity $\Delta\cdot\Xi$ is a vertically integrated diffusivity model for a Bingham-like non-Newtonian material and it is a function of a quantity $\Delta \equiv h_r - h_{45}/\tan\theta$, *which must be greater than zero*, otherwise $\Delta \equiv 0$. The angle θ describes the surface slope wherein $|\tan\theta| = |\nabla h|$. h_{45} is a constant which is a proxy for the minimum tangential stress necessary to have a non-Newtonian fluid to start flowing. The functions $\dot{h}_a, \dot{h}_w$ represent rates of local normal accretion and weathering as detailed in [5]. We have also included a scouring model representing the erosional conversion of bedrock by overlying moving regolith in which the rate of transformation is in proportion (measured by the constant τ_0) to *the traffic flow,* defined as $|\mathbf{q}|$. We note that we have also exam-

ined a parallel Glen-Law model, but this will be detailed in an upcoming paper.

We have adapted MARSSIM [5] to handle both kinds of nonlinear creeping flows described above. To verify the results garnered through MARSSIM, we have also developed the hybrid finite-difference spectral code "HGEM" to model the equation set (1.1). The details of this algorithm will also be described in an upcoming paper.

Results thus far. Fig. 2. depicts a surface relief map of the cratered initial surface in which the various scenarios are examined. All scenarios have the non-Newtonian mass flow process active.

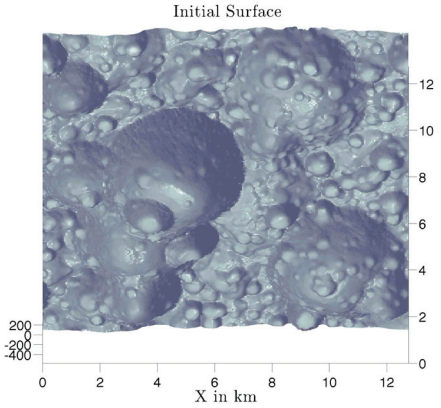

Fig. 2. Vertical scale of relief map in meters.

1. Basin filling. Early indications show that a scenario where mass transport due to non-Newtonian dynamics is shaped by the processes of weathering and accretion. Fig. 3 depicts the results of a pair of parallel runs (for arbitrarily chosen values of flow diffusivity scaling). In one case micrometeorite weathering acts alone while in the other it is supplemented by an accretion rate that is one third the weathering rate. The case in which weathering and accretion occurs in tandem shows efficient transport and basin filling. These latter simulations also show efficient crater wall retreat (not shown here).

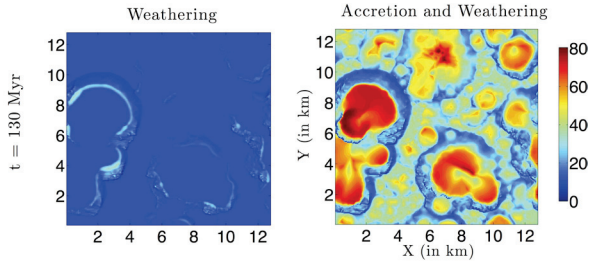

Fig. 3. Comparsion of two steady evolutionary scenarios. Plotted is the surface regolith pattern. Left panel involves weathering and nonlinear mass transport. Right panel is like the left but with accretion included. Scale in meters.

2. Surface flow patterns. We have examined the result of a scenario in which a catastrophic liberation (uniform 6 m with respect to surface normal) of the surface bedrock is followed by steady surface weathering. Fig. 4 depicts the nearly quasi-steady flow pattern that emerges after some period of adjustment. The emergence of flow lanes is clearly apparent. Flow into the three major basins are self-evident (c.f. Fig. 2).

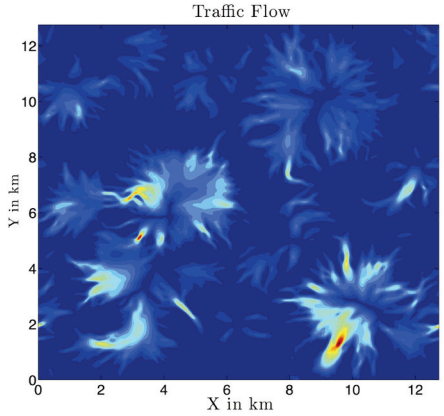

Fig. 4. Traffic flow after catastrophic liberation of regolith from surface. Deep blue indicates no flow while red indicates relatively high flow.

3. *Nonsteady activity.* In most simulations involving Bingham-flow, the time series of the flow activity over the whole surface (e.g. its surface average) shows non-steady behavior in which periods of relative quiescence are punctuated by short periods of strong readjustment. These events correspond to localized transitions in which previously Bingham static localized regolith patches exceed the minimum tangential shear threshold necessary for mass transport to occur (i.e. the regolith height increases sufficiently so that the quantity $\Delta > 0$).

Tentative conclusions: Our current examinations seem to indicate that scenarios in which accretion and weathering are both acting together can efficiently convert crater rims and transport them into crater basins. Strong crater rim retreat is observed on steep walls. The time series of surface activity is chaotic suggesting that the processes taking place on such a body may not necessarily be steady. Further scenario explorations are ongoing.

References:. [1] Thomas, P.C. et al. (2013) *Icarus 226,* 999-1019. [2] Horanyi, M. et al. (2009) in *Saturn from Cassini-Huygens*, eds. Dougherty, M.K. et al. (Springer) 511-536. [3] Hirata, N., and H. Miyamoto (2012), , *JGUM 2012*, Abstract U02-P04. [4] Wyrick, D. *private communication.* [5] Howard, A. D. (2007) *Geomorphology 91*, 332-363 (1973) *Icarus*, *18*, 224-236.